Nano Research

ISSN 1998-0124 CN 11-5974/O4
https://doi.org/10.1007/s12274-022-4692-9

Research Article

Super-assembly of integrated gold magnetic assay with loop-mediated isothermal amplification for point-of-care testing

Jianping Liang[1,§], Jie Zeng[3,§], Xiaojuan Huang[1], Tengteng Zhu[1], Yonglong Gong[1], Chen Dong[1], Xiangrong Wang[1,5], Lingzhi Zhao[1], Lei Xie[3], Kang Liang[6], Qiongxiang Tan[1], Yali Cui[1,2] (✉), Biao Kong[3] (✉), and Wenli Hui[1,4] (✉)

[1] *The College of life science, Northwest University, Xi'an 710069, China*
[2] *Shaanxi Provincial Engineering Research Center for Nano-Biomedical Detection, Xi'an 710077, China*
[3] *Department of Chemistry, Shanghai Key Lab of Molecular Catalysis and Innovative Materials, Collaborative Innovation Center of Chemistry for Energy Materials, Fudan University, Shanghai 200438, China*
[4] *Key Laboratory of Resource Biology and Biotechnology in Western China, Ministry of Education, Northwest University, Xi'an 710069, China*
[5] *Provincial Key Laboratory of Biotechnology of Shaanxi Province, Northwest University, Xi'an 710069, China*
[6] *School of Chemical Engineering, Graduate School of Biomedical Engineering, and Australian Centre for NanoMedicine, University of New South Wales, NSW 2052, Australia*
[§] *Jianping Liang and Jie Zeng contributed equally to this work.*

Received: 25 May 2022 / **Revised:** 21 June 2022 / **Accepted:** 21 June 2022

ABSTRACT

With the increasing global threat of various diseases and infections, it is essential to develop a fast, low-cost, and easy-to-use point-of-care testing (POCT) system for inspections at all levels of medical institutions and self-examination at home. In this work, gold magnetic nanoparticles (GMNPs) are used as the key material, and a rapid visual detection method is designed through integrating loop-mediated isothermal amplification (LAMP) and lateral flow assay (LFA) biosensor for detecting a variety of analytes which includes whole blood, buccal swabs, and DNA. It is worth to note that the proposed method does not need DNA extraction. Furthermore, uracil DNA glycosylase (UDG) is employed to eliminate carrier contamination for preventing false positive results. The whole detection process can be finished within 25 min. The accuracy of detection is measured by assessing the polymorphisms of the methylenetetrahydrofolate reductase (MTHFR) C677T. The detection limit of the newly developed extraction-free detection system for MTHFR C677T is 0.16 ng/μL. A preliminary clinical study of the proposed method is carried out by analyzing 600 clinical samples (including 200 whole blood samples, 100 buccal swabs, and 300 genomic DNA samples). The results indicate that the proposed method is 100% consistent with the sequencing results which provides a new choice for POCT and shows a broad application prospect in all levels of medical clinics and at home.

KEYWORDS

gold magnetic nanoparticles, loop-mediated isothermal amplification, lateral flow assay system, free extraction, single-nucleotide polymorphisms genotyping

1 Introduction

Numerous studies have shown that single-nucleotide polymorphism (SNP) is closely related to the occurrence and development of many diseases [1, 2]. There are many detection techniques currently, such as sequencing [3], DNA microarray [4], real-time polymerase chain reaction (RT-PCR) [5], and multiplex PCR-restriction fragment length polymorphism (RFLP) [6], which have their own merits and drawbacks. All of these techniques require expensive and delicate instruments, which limits their widespread application in grading diagnosis and treatment [7, 8]. Therefore, it is necessary to develop a rapid, highly accurate, and highly sensitive point-of-care testing (POCT) system for the detection of SNP in home and clinical settings.

Loop-mediated isothermal amplification (LAMP) [9] is a rapid gene amplification method which has attracted widespread attention from researchers. In this technique [9, 10], four or six primers are designed for six or eight regions of the target gene to react at isothermal conditions under the action of strand replacement DNA polymerase. Furthermore, additional loop primers are designed for speeding up the reaction [10]. In recent years, the LAMP method for efficient detection of pathogenic microorganisms and SNP has received significant attention [11–15]. LAMP has shown a high potential in molecular diagnosis because of its high sensitivity, high amplification rate, and good specificity, and has higher accuracy than other amplification methods such as PCR due to the exquisite design of primer [16].

Early LAMP detection methods for SNP include instrumental detection of specific fluorescence signals, colorimetric determination relying on fluorescent dyes, gel electrophoresis analysis, and turbidity interpretation based on pyrophosphate ion by-products [17–22]. In one work [23], Zhang et al. presented a novel method of LAMP based on fluorescence for SNP genotyping. Our investigation indicates that there still exist many interfering substances in the amplification products for whole

Address correspondence to Yali Cui, yalicui@nwu.edu.cn; Biao Kong, bkong@fudan.edu.cn; Wenli Hui, huiwl@nwu.edu.cn

blood samples (e.g., heme) which will affect with the fluorescence signal, color change, and turbidity, and hinder the direct amplification of the whole blood sample without DNA extraction. Gel electrophoresis cannot meet the requirements of POCT strategy because of complicated steps and long time. Gold magnetic nanoparticles (GMNPs) combined with LAMP can solve whole blood direct enlargement without extracting DNA to achieve one-step detection. GoldMag not only has the characteristics of high surface volume ratio and good stability of magnetic particles, but also has good biocompatibility and surface plasmon resonance optical properties of gold nanoparticles, and is easy to combine with biomolecules and modify without coupling agent. Our investigation also indicates that the extraction-free detection system based on LAMP combined lateral flow assay (LFA) system with GoldMag as carrier has not been reported.

C677T is the most common SNP in the gene of methylenetetrahydrofolate reductase (MTHFR), which is a key enzyme in folate metabolism [24]. MTHFR gene mutation can affect enzyme activity, leading to abnormal folate metabolism and reducing active folate levels, resulting in an increased risk of many diseases, such as cancer, birth defects in newborns, infertility, and cardiovascular and cerebrovascular diseases [25–31]. Therefore, it is necessary to detect the polymorphisms of MTHFR C677T gene.

In this work, with MTHFR 677 C > T as the model, a genotyping technology platform based on extraction-free LAMP combined GoldMag LFA is established. The composite has both the optical properties of colloidal gold surface plasmon resonance and the superparamagnetization of magnetic nanoparticles, which has been successfully used in targeted drug delivery, nucleic acid purification, and gene detection [32–34]. Here, Fe_3O_4/Au/Fe_3O_4 nanoparticles with hydrodynamic diameter of about 100 nm were synthesized, which were modified by poly(sodium-p-styrenesulfonate) (PSS) and coupled with antibodies as the detection carrier. In addition, the modified GoldMag has good monodispersibility, stability, and biocompatibility which can be well applied for the LFA detection of SNP. In order to prevent false positive results, we introduced uracil DNA glycosylase (UDG) for eliminating carrier contamination. The rapid and high sensitivity genotyping technology can be finished within 25 min that can be widely used in clinics and at home.

2 Experimental section

2.1 Materials and reagents

Anti-digoxin antibody was obtained from Meridian Life Science, Inc. (Saco, ME, USA). Streptavidin was purchased from Promega Biotech Inc. (Madison, WI, USA). Goat anti-mouse IgG was obtained from Joey Bioscience Inc. (Shanghai, China). Isothermal master mix was acquired from OptiGene Ltd., UK. All primers were synthesized by Invitrogen (Shanghai, China).

2.2 Modification of Gold magnetic nanoparticles by PSS and antibody coupling

The synthesis and characterization of GMNPs followed our previous study [35], and the transmission electron microscopy (TEM) image of the structural characterization is shown in Fig. 2(d). The surface of GMNPs was rich in cetyltrimethylammonium bromide (CTAB), with positive charge, while PSS had negative charge. This modification method wraps PSS on the surface of GMNPs through electrostatic adsorption under the condition of ultrasonic stirring to form negatively charged PGMNPs, and zeta potential diagram is shown in Fig. 2(b). The specific functionalization of CTAB and modification of PSS were as follows. Firstly, 30 mg acid-treated GMNPs were diluted to 5 mg/mL with ultra-pure water. After ultrasonic treatment for 20 min, CTAB with an equal volume of 50 mmol/L was added for 30 min of ultrasonic treatment. Next the supernatant was discarded after magnetic separation, and the remaining magnetic beads were washed three times with ultrapure water. Then 6 mL 10 mg/mL PSS was added with ultrasonic treatment for 30 min and the reaction was carried out for 120 min. Finally, the gold nanoparticles were placed in 7 mL of ultrapure water.

1 mg GMNPs modified PSS (PGMNPs) were placed in a 2 ml centrifuge tube, centrifuged at 6,000 rpm at 4 °C for 10 min to discard the supernatant, and then suspended with 600 μL 0.1M PB buffer containing 140 μg anti-digoxin antibody. At this time, the concentration of antibody (denoted as pre) was recorded. After the reaction at 180 rpm for 1 h, the supernatant (denoted as post) was separated and reserved by adding 600 μL 0.5×PBST and then placed in a shaking bed at 22 °C for 10 min at 180 rpm. The supernatant (denoted as Wash1) was washed and reserved and washed again (denoted as Wash2). Finally, the cleaned gold nanoparticles labeled with anti-digoxin antibody were stored in 0.5×GB buffer at 2–8 °C for later use.

Calculation of the coupling efficiency of anti-digoxin antibody on magnetic particle surface [36]

$$\text{Antibody coupling rate}\ (\%) = \frac{OD_{pre} - OD_{post} - OD_{wash}}{OD_{pre}} \times 100\%$$

2.3 Lateral flow assay device

Goat anti-mouse IgG was diluted to 2 mg/mL with 0.1 M PB buffer as the control line (C line). Streptavidin was diluted to 1 mg/mL with 0.1 m PB buffer as the test line (T line). The gold jet scribing instrument was used to spray streptavidin and goat anti-mouse IgG at a rate of 1 μL/cm on the membrane as the test line and the control line, and the interval between the test line and the control line was 0.5 cm. PGMNPs were conjugated with anti-digoxin antibody and dispersed in 0.5×GB buffer solution. The gold magnetic particles were sprayed on the nitrate fiber membrane at a speed of 10 μL/cm, and finally assembled the conjugate pad position with LFA strip.

2.4 Primer design and synthesis

The sequence of MTHFR C677T mutation site was downloaded from NCBI database (GenBank ID: 1801133). In terms of the design principle of the LAMP primers, a set of primers for LAMP were designed which include two outer primers (F3 and B3), four inner primers including two wild-type primers (FIP-WT, BIP-WT) and two mutant primers (FIP-M, BIP-M) that recognize six distinct regions of each target gene, and one loop primer for increasing the amplification rate. The variation site bases were introduced at the 5'-end of FIP and BIP primers for the 677 (C > T) site. In order to effectively enhance the specificity of primers, mismatched bases of different intensities were introduced. The 5'-end of the inner primer in the upstream of the primer group was labeled with biotin and the 5'-end of the downstream loop primer was labeled with digoxin. The designed primers were compared with BLAST sequences to confirm the specificity of the primer group. The primer sequences are shown in Table S1 in the Electronic Supplementary Material (ESM).

2.5 Sample preparation

Whole fresh human blood was collected with the fully informed consent from Chinese volunteers at the Shaanxi provincial people's hospital (Xi'an, China). Buccal swabs were obtained from 100 Chinese volunteers at Northwest University (Xi'an, China) with

the fully informed consent. The fresh whole blood was treated with alkaline solution before performing whole blood LAMP amplification without DNA extraction. Fresh whole blood samples were collected, followed by mixing of the samples with alkaline solution in a 1:2 ratio, with a final volume of 15 μL, and incubated at room temperature for 2 min. Meanwhile, the genomic DNA was extracted from matched fresh human whole blood using a whole blood genomic DNA purification kit from Xi'an gold magnetic nano biotechnology Co., LTD.

2.6 Optimization of the extraction-free LAMP-LFA

In order to prevent pollution caused by LAMP lid opening, dTTP in dNTP mixture was partially replaced by deoxyuridine triphosphate (dUTP), and UDG enzyme was added for eliminating degradation of uracil-labeled LAMP amplicons [37]. The UDG-LAMP assay was carried out in a 25 μl reaction mixture consisting of 15 μL of isothermal master mix, 1 U UDG enzyme with different amounts at 0.25, 0.5, and 0.75 μL, 25 mM dUTP (different amounts at 0.7, 1.4, and 2.8 μL), 5 μL of primer mix consisting of five primers each for F3 and B3 primers at certain concentration, FIP and BIP primers at certain concentration, LB primer at certain concentration, 1 μL sample treated solution, and ddH_2O up to 25 μL.

To determine the best working conditions, the detection system was performed with different combinations of primer ratios (i.e., FIP/BIP:F3/B3:LB at 8:1:4 and 4:1:2) and primer concentrations (i.e., 0.2 μM FIP/BIP, 0.05 μM F3/B3, and 0.1 μM LB; 0.4 μM FIP/BIP, 0.1 μM F3/B3, and 0.2 μM LB; 0.8 μM FIP/BIP, 0.2 μM F3/B3, and 0.4 μM LB; and 1.2 μM FIP/BIP, 0.3 μM F3/B3, and 0.6 μM LB) for determining the best primer concentration. The reaction mixture was incubated at 40 °C for 5 min and then further incubated at 59, 61, 63, 65, and 67 °C for 25 min, respectively.

2.7 Clinical application of the extraction-free LAMP-LFA system

300 whole blood and swab samples were used for further verifying the accuracy of the experimental results. Genomic DNA was also used as a template for 300 clinical samples. Appropriate ethical and governance permissions were obtained from the local authorities prior for blood sample collection. Moreover, 200 cases were selected for sequencing (Beijing Genomic Institute, Beijing, China).

2.8 Characterization

The size distribution and zeta potential of GMNPs, PGMNPs, and PGMNPs-anti-Dig were determined by dynamic light scatterometer (DLS) (Malvern Zetasizer Nano-ZS, Malvern Instrument, Worcestershire, UK). TEM (Hitachi H-600, Hitachi Corporation, Japan) was used to obtain particle images for structural evaluation. Fourier transform infrared spectroscopy (FTIR, Thermo Nicolet 5700, Thermo Nicolet Corporation, USA) was used for characterizing the prepared magnetic particles. Ultraviolet–visible (UV–Vis) spectroscopy was recorded in the wavelength range of 200–700 nm using a UV-2550 spectrophotometer (Shimadzu, Japan). The gold jet scribing instrument (BioDot Corporation, USA) was used to spray streptavidin, goat anti-mouse IgG, and PGMNPs-anti-Dig.

3 Results and discussion

3.1 Assembly and modification of GMNPs

Toward the design of an effective nanomaterial assisted detection system, the key material of LFA system is GMNPs with good superparamagnetism and biocompatibility. As shown in Fig. 1(a), GMNPs are functionalized with CTAB surfactants, next modified with PSS, and the modified GMNPs (PGMNPs) are conjugated with anti-digoxin antibody by physical adsorption. PSS has a very strong negative charge, so the steric hindrance and electrostatic repulsion between nanoparticles, and its corresponding monodispersity and stability can be effectively enhanced when PSS is coated on the surface [38, 39].

PSS modified gold magnetic particles were coupled with anti-digoxin antibody and dispersed in 0.5×GB buffer solution. The gold spraying apparatus was used to spray the particles on cellulose nitrate film at a speed of 10 μL/cm, and finally assembled on the conjugate pad of LFA strip (Fig. 1(b)). Due to the high adhesion for antibodies and good dispersion of the surface of the nanoparticles, it can be combined with the target molecule labeled digxin and biotin (Fig. 1(c)) and coupled in the detection of T-line

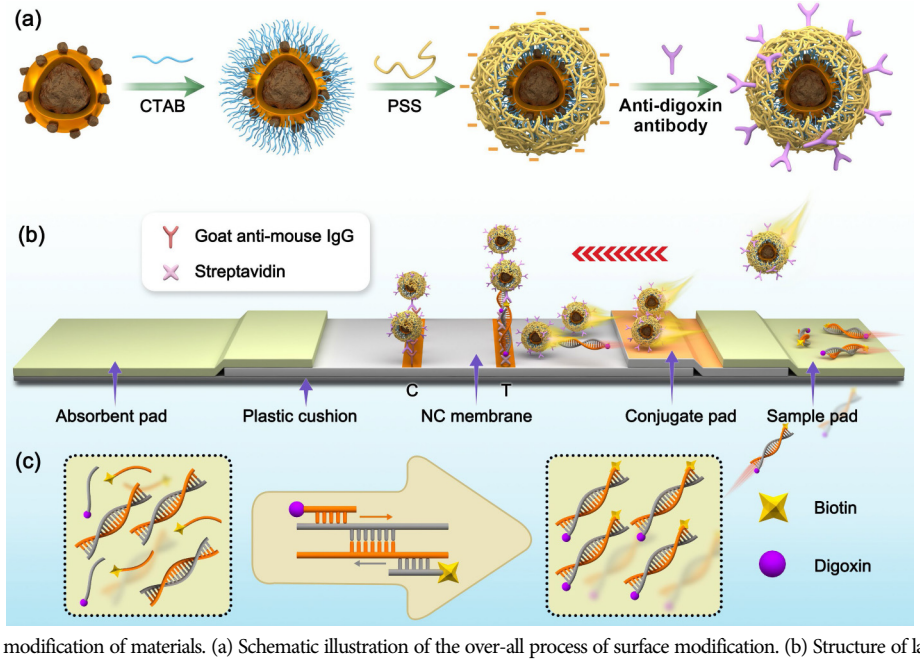

Figure 1 Assembly and modification of materials. (a) Schematic illustration of the over-all process of surface modification. (b) Structure of labeled lateral flow device. (c) The marker of primer sets and amplification of target sequence.

color (Fig. 1(b)).

As illustrated in Fig. 1(b), the LFA device was performed over a strip, which was composed of five overlapping pads, i.e., sample pad, conjugate pad, nitrocellulose membrane, absorbent pad, and plastic cushion. Goat anti-mouse IgG and streptavidin were pre-immobilized in the C line and T line on a porous nitrocellulose membrane. Then, PGMNPs coupled with anti-digoxin antibody were sprayed on conjugated pads of LFA bands in order to combine with subsequent products for SNP detection. As shown in Fig. 1(c), the internal primer and loop primer were labeled with biotin and digoxin respectively, so the double labeled product and anti-digoxin antibody on PGMNPS formed a composite probe for visual detection on LFA as illustrated in Figs. 3(a) and 3(c).

3.2 Characterization of GMNPs

The synthesis and characterization of GMNPs have been discussed in detail in our previous studies [1]. The TEM image of the structural characterization of GMNPs is shown in Fig. 2(d). Successful modification of GMNPs was confirmed by the FTIR spectra and the characteristic peaks were identified. The FTIR spectra of the Fe_3O_4/Au/Fe_3O_4 nanoparticles after modification by PSS are shown in Fig. 2(a). The characteristic peak at 585 cm^{-1} is related to Fe–O bond in GMNPs [40]. The characteristic absorption bands of 1,037 and 1,637 cm^{-1} correspond to the symmetric vibration of the sulfonate group (SO_3^-) and the stretching vibration of C=C of Benzene [41]. As shown in Fig. 2(b), the GoldMag modified by PSS was negatively charged, while the GMNPs were positively charged. All of these prove that PSS is successfully attached to the surface of nanoparticles. Moreover, the high zeta potential confirmed that the stability and dispersion of the nanoparticles were maintained due to the mutual repulsion between PGMNPs with high negative charge [38, 39].

GMNPs are a nanocomposite composed of colloidal gold and Fe_3O_4 with a particle size of about 40 nm (Fig. 2(d)). The hydrated particle size of GMNPs is about 149.8 nm (Fig. 2(c), black column). After PSS modification, the hydrated particle size is 103.2 nm (Fig. 2(c), PGMNPs red column). The hydration particle size after modification is smaller than that before modification, which is caused by the agglomeration of some GMNPs nanoparticles before modification and some dispersion after PSS modification. As can be seen from the PDI dispersion during particle size analysis, the PDI value was 0.259 nm before modification and 0.116 nm after modification. Finally, after antibody coupling, the hydrated particle size increased to 267.3 nm (Fig. 2(c)), indicating that the antibody successfully combined with magnetic bead PGMNPs, and the hydrated particle size could meet the requirements of LFA detection system.

Because of the optical properties of gold particles, the monodispersity of gold nanoparticles can be characterized by observing the position and intensity of UV–Vis spectroscopy at 350–750 nm. By measuring UV–Vis, the absorption peak should be the characteristic absorption peak of nanogold in the composite material. For nanogold with smaller particle size, the absorption peak position is smaller. The absorption peak position of GMNPs is 552 nm, which is 540 nm after PSS modification (Fig. 2(e)). The reason may be that some nanoparticles agglomerate in unmodified GMNPs, resulting in larger absorption peaks. After PSS modification, the dispersion of PGMNPs becomes better under the action of strong surface charge and spatial resistance of surface modified molecules, resulting in blue shift of UV absorption peak. This result is also consistent with particle size analysis in Fig. 2(c). After PSS modification, the antibody was coupled and the characteristic absorption peak after coupling was 544 nm (Fig. 2(e)). Meanwhile, there was also a characteristic peak at 280 nm (Fig. 2(e)), which was because there were more anti-digoxin antibodies enriched on the surface of PGMNPs. Therefore, this peak was analyzed as the characteristic peak of anti-digoxin antibodies.

During the experiment, the use of weakly alkaline pH buffer resulted in a higher antibody coupling amount. The reason is that the antibodies would change from dissolved to aggregated state near the isoelectric point [42]. In this way, the antibodies have the strongest hydrophobicity and bind stronger to the hydrophilic PGMNPs. In terms of the formula of antibody coupling rate, 120 μg anti-digoxin antibody could be conjugated on the surface of 1 mg magnetic particles. The coupled magnetic beads are stored in GB buffer which plays a sealing and protection role. The material, its modification and antibody coupling were analyzed

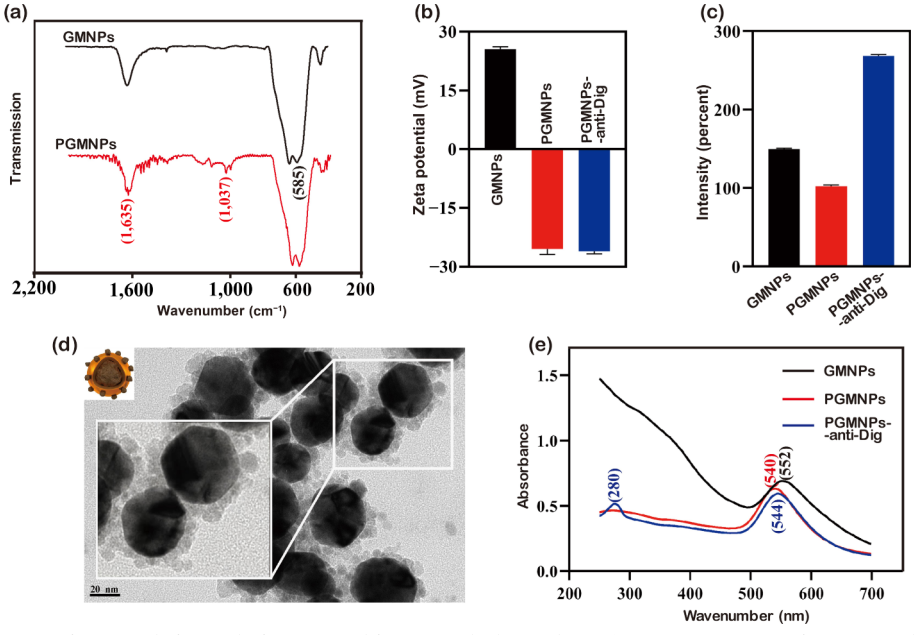

Figure 2 The characterization of GMNPs before and after PSS modification antibody coupling. (a) FTIR spectroscopy of GMNPs and PGMNPs. (b) The zeta potential distributions of GMNPs, PGMNPs, and PGMNPs-anti-Dig. (c) The size distributions of GMNPs, PGMNPs, and PGMNPs-anti-Dig. (d) TEM image of GMNPs. (e) The UV–Vis spectroscopy of GMNPs, PGMNPs, and PGMNP-anti-Dig. The concentration of GMNPs used for measurement was 0.50 mg/mL. The concentration of PGMNPs was 0.40 mg/mL. The concentration of PGMNPs-anti-Dig was 0.35 mg/mL.

and discussed above. Finally, PGMNPs material with antibody was used in downstream LFA system. The average pore size of NC membrane by double antibody sandwich method in LFA system is about 8 μm. After analysis and discussion, PGMNPs can meet the following application research.

3.3 Design of the extraction-free LAMP-LFA system

The principle of the extraction-free detection system is schematically illustrated in Fig. 3. Since LAMP is targeted at the gene detection of SNP sites, it is difficult to ensure its specificity. A unique primer design scheme was adopted in this study as show in Fig. 3(a). According to the point mutation of MTHFR C677T, five specific primers have been designed. Since LAMP amplification depended on specific primers, the SNP site was located at the 5'-end of the FIP and BIP. Each reaction consisted of two common primers (F3 and B3), loop primers, and two special primers (FIP-WT and BIP-WT for wild-type alleles, and FIP-M and BIP-M for mutant alleles). The target fragment amplification occurs only when the 5'-end of the specific primer is complementary with the template. In order to further improve the specificity of the primers [43, 44], base mismatch was introduced in the penultimate position of the 5'-end of the specific primers.

Two separate LAMP tubes are required for determining the genotype of each sample (i.e., M tube and WT tube). Fresh whole blood samples treated with 0.1% NaOH, buccal swabs, and genomic DNA were used as templates for amplification within two tubes as shown in Fig. 3(b). Pretreatment of the samples with alkaline solution is crucial for this method [45–47]. In our system, the alkaline solution can effectively induce cell lysis and achieve DNA release, saving the time of DNA extraction from the sample without DNA loss, making the whole detection process more convenient and faster. The electrostatic interaction between proteins and genomic DNA was effectively weakened after alkali treatment, enabling the release of tightly bound DNA from chromatin [48]. Unlike the fluorescence signal and turbidity, the LFA system is not affected by heme because the sample pad and conjugate pad can effectively filter the interfering substances in the amplification products.

As shown in Fig. 3(c), LAMP double-labeled amplification products formed by biotin and digoxin labeled at the 5'-end of the internal primer and loop primer are added to the sample pad, and the results are visually read within 5 min. Digoxin labeled on 5'-end is recognized and captured by PGMNPs-anti-Dig on the conjugate pad to form LAMP product-PGMNPs composites. Then the biotin labeled end is bound to the streptavidin at the T line when the composites migrate to T line, thus forming a visible red band here. The remaining PGMNPs-anti-dig moves further to bind to goat anti-mouse IgG at the C line, also showing red bands as confirmation of the validity of the strip. The T line does not display red strip when there is no LAMP product. For the

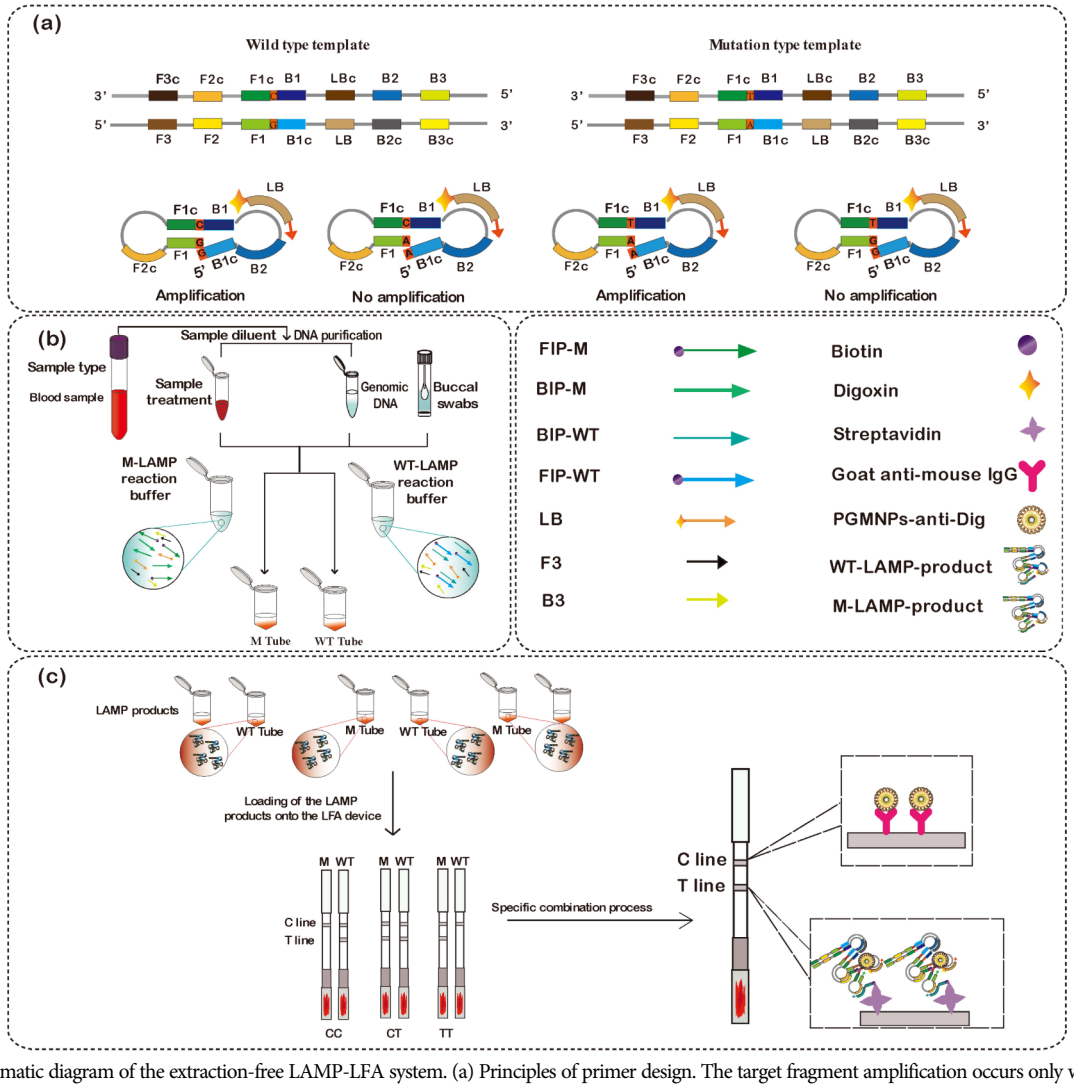

Figure 3 Schematic diagram of the extraction-free LAMP-LFA system. (a) Principles of primer design. The target fragment amplification occurs only when the 5'-end of the specific primer is complementary with the template. (b) Sample preparation and target amplification. (c) The LFA schematic diagram for genotyping result of homozygous, heterozygous, and wild type samples by extraction-free LAMP-LFA. M = M tube. WT = WT tube.

homozygous sample (TT), a distinct red band was observed on the T line of the strip used only for the M tube but not for the WT tube. In contrast, for the wild-type sample (CC), the red band showed exclusively on the strip receiving the WT tube but not the M tube. However, red bands with similar intensities on the T lines of both strips indicated a heterozygous sample (CT).

3.4 Optimization of the extraction-free LAMP-LFA system

Although LAMP method is known for its unique advantages, its high amplification efficiency will inevitably increase the risk of contamination and easily lead to false positive results. The reason is that the LAMP products in the early stage of detection can easily re-enter the tube and become the template for re-amplification, that is, the pollution carried by aerosol droplets [37, 49], while such contamination can be effectively eliminated by introducing dUTP and UDG. UDG is a DNA repair enzyme that cleaves the N-glycoside bond between the uracil base and deoxyribose of DNA, but has no activity against the four other common nucleotide residues. Therefore, dUTP is integrated into the amplicon through N-glycoside bond, and in the next LAMP reaction, the amplicon (aerosol pollutant) is cleaved by UDG, and the resulting pyrimidine-free sites and UDG are hydrolyzed and inactivated at high temperature, thus eliminating the false positives generated by pollution [50].

The LAMP reaction using dUTP instead of dTTP and UDG progressed well, and the concentration of dUTP affected the reaction rate [51, 52] as shown in Fig. 4(a). When the content of dUTP was 2.8 μL, no bands appeared on the strip (Fig. 4(a), lane 3). We also experimented on the content of UDG enzyme and found that the amount of enzyme had no effect on the reaction rate (Fig. 4(b)) [53]. Therefore, when the content of dUTP was 0.7 μL, the content of UDG was 0.5 μL, which was chosen for the subsequent UDG-LAMP assays to study the specificity and sensitivity.

To evaluate the ability of UDG-LAMP assay to prevent carry-over contamination, we used a LAMP product with continuous dilution from the previous reaction amplification as a template for the reaction. After treatment at 40 °C for 5 min, the LAMP reaction was put into the instrument at 61 °C for 25 min. In the experiment without UDG, each reaction could be amplified in the reaction tube containing pre-amplified DNA (Fig. 4(c)). The results illustrated the risk of contamination in reactions, where even small amounts of any contaminant may cause unnecessary amplification. In contrast, when contaminated DNA was diluted to 10^{-8} in LAMP, UDG treatment prevented amplification (Fig. 4(d), lane 1). This showed that the method can prevent typical aerosol-based pollution [54].

The specificity of the extraction-free LAMP-LFA system was

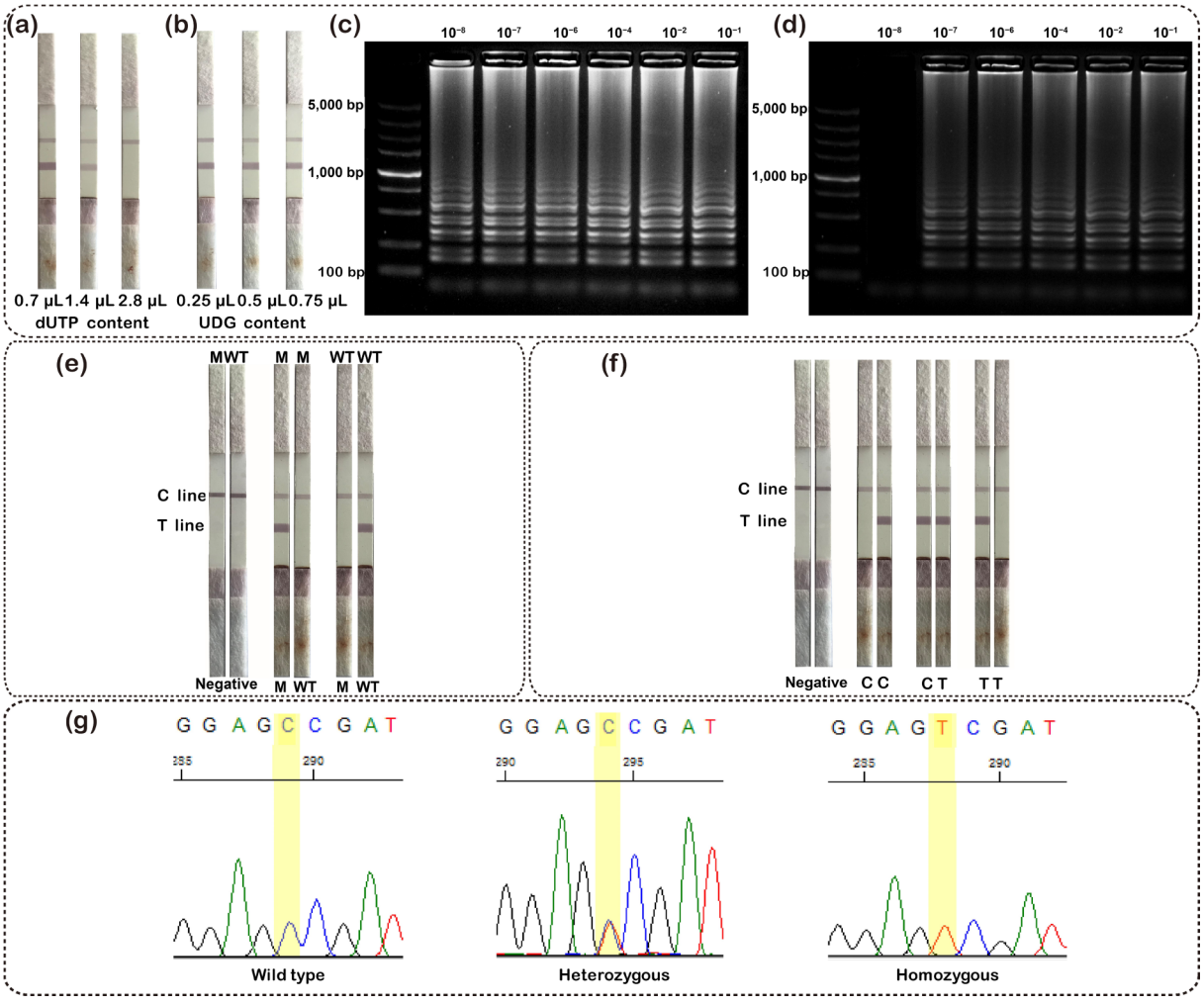

Figure 4 The results of the optimization of each content in the reagent and the verification of pollution prevention. (a) The concentration of dUTP. (b) The concentration of UDG enzymes. (c) The amplification results of UDG were not added. (d) The effect of UDG that was used to prevent contamination. (e) The specificity of the extraction-free LAMP-LFA system. M: Mutation primer set; WT: Wild type primer set; m: Mutation template; and wt: Wild type template. (f) The genotyping results of wild type, heterozygous, and homozygous samples by extraction-free LAMP-LFA system. (g) The sequencing results for MTHFR C677T genotyping.

assessed, and cross-experiments were conducted in the wild-type and mutant primer groups, using the samples of known homozygous mutant and homozygous wild-type as templates. The results in Fig. 4(e) (Fig. S1 in the ESM) showed that the system had good specificity. The results of the three genotypes are shown in Fig. 4(f) (Fig. S2 in the ESM), and were compared with sequencing (Fig. 4(g)).

To determine the optimal conditions for UDG-LAMP assay, whole blood samples of three different genotypes of MTHFR C677T were used for LAMP detection at different primer concentrations and reaction temperatures. The best amplification efficiency and specificity were obtained when the primer ratio was 4:1:2 (Fig. S3(a) in the ESM). The optimal primer concentration combination was 0.8 μM of the FIP/BIP, 0.2 μM of the F3/B3, and 0.4 μM of the LB (Fig. S3(b) in the ESM). In addition, the best reaction temperature was 61 °C (Fig. S3(c) in the ESM).

3.5 Evaluation of the extraction-free LAMP-LFA system

To evaluate the performance of extraction-free detection system, the sensitivity of LFA was tested using various quantities of whole blood samples with known MTHFR genotypes. Gradient dilution of whole blood with physiological saline was conducted at 1:1, 1:59, 1:79, 1:99, 1:109, 1:119, 1:139, 1:159, 1:179, and 1:199 ratios. The sensitivity detection results of whole blood are shown in Fig. 5. Compared with the traditional PCR detection method, the sensitivity is 31 times higher [55]. Blood routine tests were performed in the People's Hospital of Shaanxi Province. The cell count results of the samples at different dilution ratios are shown in Fig. 5 and summarized in Table S2 in the ESM. The amount of nucleic acid in a white blood cell is 6.25 pg [56]. The results indicate that the minimum detection sensitivity is 0.16 ng/μL (Fig. 5).

Compared with the existing methods, the proposed method has higher sensitivity of extraction-free LAMP-LFA system. The reason is that the higher specific surface area of the magnetic beads has the ability to enrich the labeled target antibody and effectively improve the sensitivity of the detection system. Since gold magnetic nanoparticles are gold-coated Fe_3O_4 complex, the composite has good color development results in T line, and can be clearly detected by visual inspection.

3.6 Clinical application of the extraction-free LAMP-LFA system

In clinical practice, the presence of some endogenous substances in whole blood will interfere with the results of the system. In this study, 6 high bilirubin, 6 high cholesterol, and 6 hemolysis samples were taken as clinical whole blood samples for verifying the anti-interference ability of the system. As shown in Fig. 5, all the detection rates of hyperbilirubin samples, hypercholesterol samples, and hemolysis samples of known genotypes (CC, CT, and TT) are 100%, which proved that these three interference factors had no influence on the detection process and result of

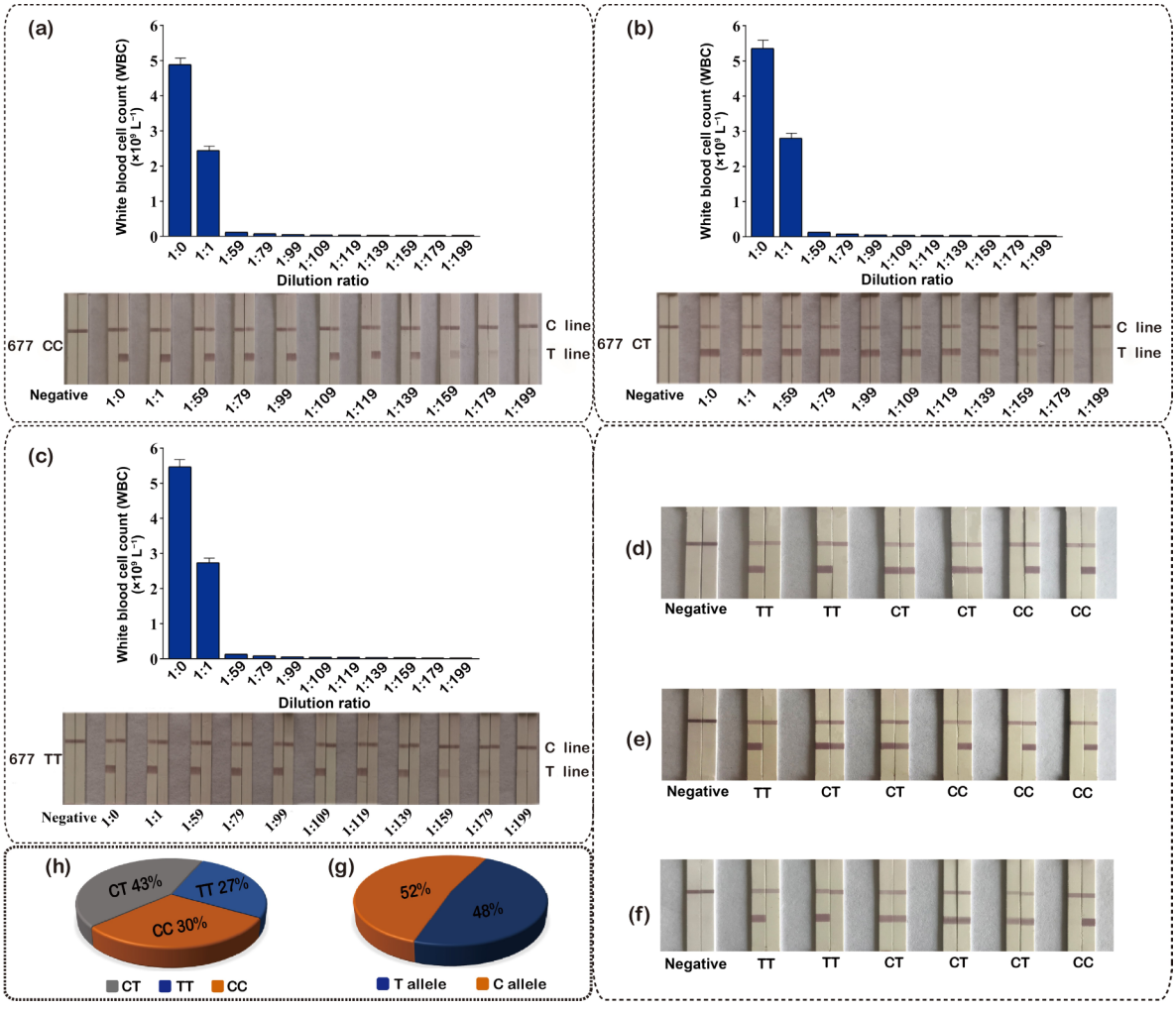

Figure 5 The sensitivity and anti-interference results of the extraction-free LAMP-LFA method and the genotype frequencies of MTHFR C677T. (a)–(c) The cell count results of wild-type samples, mutant samples, and heterozygous samples at different dilution ratios and the sensitivity analysis of the strip. (d)–(f) The results of anti-interference experiment when whole blood endogenous substances are high bilirubin, high cholesterol, and hemolysis samples, respectively. (g) The gene frequencies of the three MTHFR C677T genotypes. (h) The statistical results of the frequency of MTHFR C677T C alleles and T alleles.

whole blood samples of C677T gene polymorphism. Furthermore, it can be proved that the proposed system has good stability and can be better promoted and applied in clinical.

To evaluate the reliability of the optimized extraction-free detection system in this study, the accuracy was further verified with 600 clinical samples (200 whole blood, 100 buccal swab, and 300 genomic DNA samples) from the Shaanxi Provincial People's Hospital (Xi'an, China) with informed consent. 200 samples are randomly selected and sent them for sequencing. As shown in Table S3 in the ESM, the genotyping results of the three genotypes had a coincidence rate of 100% with sequencing results. In addition, a Hardy–Weinberg equilibrium test was performed on selected samples (Table S4 in the ESM), and analyzed the genotype and allele frequencies of 200 cases (Fig. 5). The results were consistent with the Hardy Weinberg's law of equilibrium, indicating that the selected groups of this sample are representative of the group. The genotype frequencies of MTHFR C677T CC, CT, and TT types were 30% (59 cases), 43% (87 cases), and 27% (54 cases) (Fig. 5(a)). The allele frequency for the C allele was 52% and the T allele was 48% (Fig. 5(b)), which was in agreement with those reported by Hui et al [47, 55].

The above clinical results illustrate that the detection rate of the technology platform is 100%, which is consistent with the sequencing results, and the platform has good anti-interference performance and strong effectiveness and applicability in clinical detection. Firstly, the platform uses probe dual markers combined with LFA system based on GoldMag for achieving rapid visualization of multiple types of whole blood, oral swabs, and DNA in one step. Secondly, the method realizes the detection of nucleic acid free extraction, alkaline solution can induce leukocyte lysis, effectively weaken the electrostatic interaction between protein and DNA to achieve DNA release, and can destroy the structure of the protein that inhibits amplification in the whole blood such as hemoglobin, saving the time to extract DNA from the sample. Moreover, we introduced an anti-contamination system for solving false positive caused by high amplification. This is because LAMP is labeled as uracil containing product by introducing dUTP which is cleaved by UDG through N-glycoside bond in the next round of amplification.

3.7 Mechanism investigation of PGMNPs as efficient material for LAMP-LFA system

Through the primer design and labeling of allele MTHFR C677T gene mutation site, namely, loop primer with digxin molecular labeling and internal primer with biotin molecular labeling, specific amplified fragment was obtained by LAMP amplification. The digoxin labeled product interacts with the anti-digoxin antibody on the surface of gold nanoparticles in the constructed genotyping system (Fig. 6(a)), and the biotin labeled on the primer probe binds to the streptoavidin sprayed on the detection line (Fig. 6(b)), while residual magnetic beads bind with goat anti-mouse IgG on the C line (Fig. 6(c)), so the polymorphism of MTHFR C677T gene can be detected by lateral flow assay.

Flower-shaped GoldMag is a Fe_3O_4/Au/Fe_3O_4 nanoflower complex with high specific surface area, good monodispersity, strong biocompatibility, and easy labeling of biomolecules. The structural characteristics of the material can be highly loaded with specific antibodies, which can be combined with digoxin molecule labeled products in the detection system (Fig. 6(b)), so as to achieve high sensitivity detection, detection sensitivity can reach

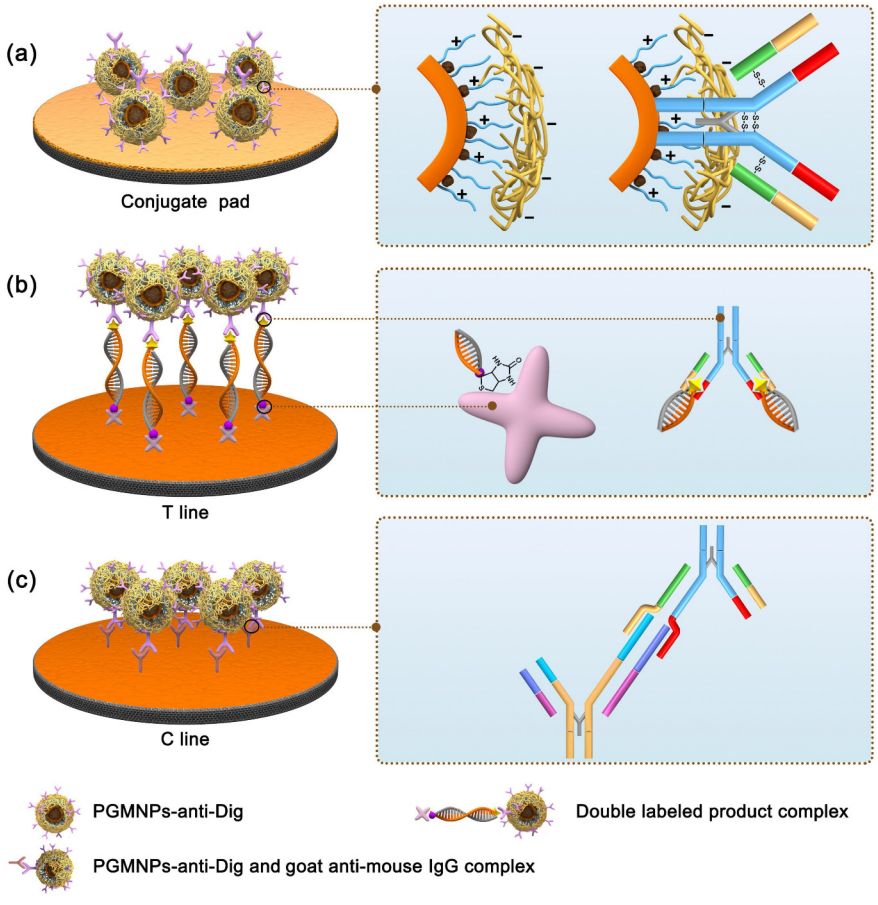

Figure 6 The detection process of lateral flow assay based on GoldMag nanoparticles. (a) PGMNPs-anti-Dig are sprayed on conjugate pad. (b) PGMNPs- anti-Dig forms a complex with the double labeled product and conjugated with streptavidin on T line via biotin. (c) The remaining PGMNPs were captured by goat anti-mouse IgG.

0.16 ng/μL.

4 Conclusions

In this study, a rapid extraction-free detection system based on super-assembled gold magnetic assay was established for detecting SNPs with multifarious sample types. This is the first report of SNP detection platform, which combines the UDG, free extraction, and LAMP-LFA for genotyping with various clinical samples validation. It has been verified that the proposed method has the ability to achieve one-step rapid direct amplification of whole blood and buccal swab without extraction within 25 min and also achieve the amplification of genomic DNA. It also has been proved that the proposed method has high specificity and sensitivity (the sensitivity can be up to 0.16 ng/μL). In this work, the dUTP-UDG system is introduced which has the ability to effectively reduce the probability of false positives caused by contamination and effectively improve the overall stability of extraction-free LAMP-LFA visual detection. Due to the high specific surface area and easy surface functionalization of magnetic beads, more target antibodies can be enriched, so the system has high sensitivity, and the detection results are fast and efficient due to its good monodispersity and stronger stability. This system provides a novel selection for the realization of point-of-care testing. It has a broad application prospect in all levels of medical institutions and home-based POCT. Moreover, due to the optical and magnetic properties of gold magnetic nanoparticles, the detection system not only can be used for visual inspection, we will also apply it to molecular diagnosis of magnetic quantitative in the future.

Acknowledgements

This work was supported by the National Natural Science Foundation of China (Nos. 31771083 and 81772289).

Electronic Supplementary Material: Supplementary material (details for MTHFR C677T primer sequences, the cell count results of samples at different dilution ratios, genotyping results and frequency samples, a Hardy–Weinberg equilibrium test, the sensitivity of the system, detection results of multiple samples, and optimization of the system) is available in the online version of this article at https://doi.org/10.1007/s12274-022-4692-9.

References

[1] Everitt, A. R.; Clare, S.; Pertel, T.; John, S. P.; Wash, R. S.; Smith, S. E.; Chin, C. R.; Feeley, E. M.; Sims, J. S.; Adams, D. J. et al. IFITM3 restricts the morbidity and mortality associated with influenza. *Nature* **2012**, *484*, 519–523.

[2] Moore, J.; McKnight, A. J.; Simmonds, M. J.; Courtney, A. E.; Hanvesakul, R.; Brand, O. J.; Briggs, D.; Ball, S.; Cockwell, P.; Patterson, C. C. et al. Association of caveolin-1 gene polymorphism with kidney transplant fibrosis and allograft failure. *JAMA* **2010**, *303*, 1282–1287.

[3] Grant, J. R.; Arantes, A. S.; Liao, X. P.; Stothard, P. In-depth annotation of SNPs arising from resequencing projects using NGS-SNP. *Bioinformatics* **2011**, *27*, 2300–2301.

[4] Li, J.; Huang, Y.; Wang, D. F.; Song, B.; Li, Z. H.; Song, S. P.; Wang, L. H.; Jiang, B. W.; Zhao, X. C.; Yan, J. et al. A power-free microfluidic chip for SNP genotyping using graphene oxide and a DNA intercalating dye. *Chem. Commun.* **2013**, *49*, 3125–3127.

[5] Martinez-Serra, J.; Robles, J.; Nicolàs, A.; Gutierrez, A.; Ros, T.; Amat, J. C.; Alemany, R.; Vögler, O.; Abelló, A.; Noguera, A. et al. Fluorescence resonance energy transfer-based real-time polymerase chain reaction method without DNA extraction for the genotyping of F5, F2, F12, MTHFR, and HFE. *J. Blood Med.* **2014**, *5*, 99–106.

[6] Loo, K. W.; Griffiths, L. R.; Gan, S. H. A novel multiplex PCR-RFLP method for simultaneous detection of the MTHFR 677 C > T, eNOS +894 G > T and - eNOS −786 T > C variants among Malaysian Malays. *BMC Med. Genet.* **2012**, *13*, 34.

[7] Hendre, P. S.; Kamalakannan, R.; Varghese, M. High-throughput and parallel SNP discovery in selected candidate genes in *Eucalyptus camaldulensis* using Illumina NGS platform. *Plant Biotechnol. J.* **2012**, *10*, 646–656.

[8] Ahsan, M.; Li, X. D.; Lundberg, A. E.; Kierczak, M.; Siegel, P. B.; Carlborg, O.; Marklund, S. Identification of candidate genes and mutations in QTL regions for chicken growth using bioinformatic analysis of NGS and SNP-chip data. *Front. Genet.* **2013**, *4*, 226.

[9] Notomi, T.; Okayama, H.; Masubuchi, H.; Yonekawa, T.; Watanabe, K.; Amino, N.; Hase, T. Loop-mediated isothermal amplification of DNA. *Nucleic Acids Res.* **2000**, *28*, e63.

[10] Nagamine, K.; Hase, T.; Notomi, T. Accelerated reaction by loop-mediated isothermal amplification using loop primers. *Mol. Cell. Probes* **2002**, *16*, 223–229.

[11] Kim, D. Y.; Kim, H. R.; Park, J. H.; Kwon, N. Y.; Kim, J. M.; Kim, J. K.; Park, J. H.; Lee, K. K.; Kim, S. H.; Kim, W. I. et al. Detection of a novel porcine circovirus 4 in Korean pig herds using a loop-mediated isothermal amplification assay. *J. Virol. Methods* **2022**, *299*, 114350.

[12] Wang, Y.; Wang, X. X.; Chen, H.; Han, L. M.; Wang, L. C.; Chen, T.; Li, S.; Li, H.; Li, Y. L.; Li, Z. K. et al. A novel real-time reverse transcription loop-mediated isothermal amplification detection platform: Application to diagnosis of COVID-19. *Front. Bioeng. Biotechnol.* **2021**, *9*, 748746.

[13] Kwon, S. J.; Cho, Y. E.; Kim, M. H.; Seo, J. K. A one-step reverse-transcription loop-mediated isothermal amplification assay optimized for the direct detection of cucumber green mottle mosaic virus in cucurbit seeds. *Mol. Cell. Probes* **2021**, *60*, 101775.

[14] Khammanee, T.; Sawangjaroen, N.; Buncherd, H.; Tun, A. W.; Thanapongpichat, S. A LAMP-SNP assay detecting C580Y mutation in *Pfkelch13* gene from clinically dried blood spot samples. *Korean J. Parasitol.* **2021**, *59*, 15–22.

[15] Cibecchini, G.; Cecere, P.; Tumino, G.; Morcia, C.; Ghizzoni, R.; Carnevali, P.; Terzi, V.; Pompa, P. P. A fast, naked-eye assay for varietal traceability in the durum wheat production chain. *Foods* **2020**, *9*, 1691.

[16] Zhang, S. N.; Cai, Y.; Zhang, J. X.; Liu, X. N.; He, L. H.; Cheng, L.; Hua, K.; Hui, W. L.; Zhu, J. L.; Wan, Y. S. et al. Tetra-primer ARMS-PCR combined with GoldMag lateral flow assay for genotyping: Simultaneous visual detection of both alleles. *Nanoscale* **2020**, *12*, 10098–10105.

[17] Komura, R.; Kawakami, T.; Nakajima, K.; Suzuki, H.; Nakashima, C. Simultaneous detection of benzimidazole-resistant strains of fusarium head blight using the loop-mediated isothermal amplification-fluorescent loop primer method. *J. Gen. Plant Pathol.* **2018**, *84*, 247–253.

[18] Tsujimura, K.; Bannai, H.; Nemoto, M.; Kokado, H. Loop-mediated isothermal amplification-fluorescent loop primer assay for the genotyping of a single nucleotide polymorphism at position 2254 in the viral DNA polymerase gene of equid alphaherpesvirus 1. *J. Vet. Diagn. Invest.* **2019**, *31*, 640–644.

[19] Mori, Y.; Kitao, M.; Tomita, N.; Notomi, T. Real-time turbidimetry of LAMP reaction for quantifying template DNA. *J. Biochem. Biophys. Methods* **2004**, *59*, 145–157.

[20] Mori, Y.; Nagamine, K.; Tomita, N.; Notomi, T. Detection of loop-mediated isothermal amplification reaction by turbidity derived from magnesium pyrophosphate formation. *Biochem. Biophys. Res. Commun.* **2001**, *289*, 150–154.

[21] Goto, M.; Honda, E.; Ogura, A.; Nomoto, A.; Hanaki, K. I. Colorimetric detection of loop-mediated isothermal amplification reaction by using hydroxy naphthol blue. *BioTechniques* **2009**, *46*, 167–172.

[22] Mohon, A. N.; Menard, D.; Alam, M. S.; Perera, K.; Pillai, D. R. A novel single-nucleotide polymorphism loop mediated isothermal amplification assay for detection of artemisinin-resistant *Plasmodium falciparum* malaria. *Open Forum Infect. Dis.* **2018**, *5*, ofy011.

[23] Zhang, C.; Yao, Y.; Zhu, J. L.; Zhang, S. N.; Zhang, S. S.; Wei, H.;

Hui, W. L.; Cui, Y. L. Establishment and application of a real-time loop-mediated isothermal amplification system for the detection of *CYP2C19* polymorphisms. *Sci. Rep.* **2016**, *6*, 26533.

[24] Nazki, F. H.; Sameer, A. S.; Ganaie, B. A. Folate: Metabolism, genes, polymorphisms and the associated diseases. *Gene* **2014**, *533*, 11–20.

[25] Frosst, P.; Blom, H. J.; Milos, R.; Goyette, P.; Sheppard, C. A.; Matthews, R. G.; Boers, G. J. H.; den Heijer, M.; Kluijtmans, L. A. J.; van den Heuvel, L. P. et al. A candidate genetic risk factor for vascular disease: A common mutation in methylenetetrahydrofolate reductase. *Nat. Genet.* **1995**, *10*, 111–113.

[26] Zhuo, X. L.; Song, J.; Li, D. R.; Wu, Y. Z.; Zhou, Q. MTHFR C677T polymorphism interaction with heavy alcohol consumption increases head and neck carcinoma risk. *Sci. Rep.* **2015**, *5*, 10671.

[27] Xuan, C.; Li, H.; Zhao, J. X.; Wang, H. W.; Wang, Y.; Ning, C. P.; Liu, Z.; Zhang, B. B.; He, G. W.; Lun, L. M. Association between MTHFR polymorphisms and congenital heart disease: A meta-analysis based on 9,329 cases and 15,076 controls. *Sci. Rep.* **2014**, *4*, 7311.

[28] He, J.; Liao, X. Y.; Zhu, J. H.; Xue, W. Q.; Shen, G. P.; Huang, S. Y.; Chen, W.; Jia, W. H. Association of MTHFR C677T and A1298C polymorphisms with non-Hodgkin lymphoma susceptibility: Evidence from a meta-analysis. *Sci. Rep.* **2014**, *4*, 6159.

[29] Holmes, M. V.; Newcombe, P.; Hubacek, J. A.; Sofat, R.; Ricketts, S. L.; Cooper, J.; Breteler, M. M.; Bautista, L. E.; Sharma, P.; Whittaker, J. C. et al. Effect modification by population dietary folate on the association between MTHFR genotype, homocysteine, and stroke risk: A meta-analysis of genetic studies and randomised trials. *Lancet* **2011**, *378*, 584–594.

[30] Li, P. P.; Qin, C. Methylenetetrahydrofolate reductase (MTHFR) gene polymorphisms and susceptibility to ischemic stroke: A meta-analysis. *Gene* **2014**, *535*, 359–364.

[31] Yan, L. F.; Zhao, L.; Long, Y.; Zou, P.; Ji, G. X.; Gu, A. H.; Zhao, P. Association of the maternal MTHFR C677T polymorphism with susceptibility to neural tube defects in offsprings: Evidence from 25 case-control studies. *PLoS One* **2012**, *7*, e41689.

[32] Lian, T.; Peng, M. L.; Vermorken, A. J. M.; Jin, Y. Y.; Luo, Z. Y.; Van de Ven, W. J. M.; Wan, Y. S.; Hou, P.; Cui, Y. L. Synthesis and characterization of curcumin-functionalized HP-β-CD-modified GoldMag nanoparticles as drug delivery agents. *J. Nanosci. Nanotechnol.* **2016**, *16*, 6258–6264.

[33] Zhang, C.; Liu, X. N.; Yao, Y.; Liu, K. W.; Hui, W. L.; Zhu, J. L.; Dou, Y. L.; Hua, K.; Peng, M. L.; Wang, Z. K. et al. Genotyping of multiple clinical samples with a combined direct PCR and magnetic lateral flow assay. *iScience* **2018**, *7*, 170–179.

[34] Zhao, M.; Zhang, X. Q.; Wang, S.; Chen, C.; Cui, Y. L. A simple method for purification of genomic DNA from whole blood using Fe_3O_4/Au composite particles as a carrier. *J. Med. Coll. PLA* **2009**, *24*, 239–243.

[35] Hui, W. L.; Shi, F.; Yan, K. P.; Peng, M. L.; Cheng, X.; Luo, Y. L.; Chen, X. M.; Roy, V. A. L.; Cui, Y.; Wang, Z. K. Fe_3O_4/Au/Fe_3O_4 nanoflowers exhibiting tunable saturation magnetization and enhanced bioconjugation. *Nanoscale* **2012**, *4*, 747–751.

[36] Hui, W. L. Fabrication of GoldMag nanoparticles-based genotyping system and its application in medication guide of clopidogrel. Ph. D. Dissertation, Northwest University, Xi'an, Shaanxi, 2013.

[37] Hsieh, K.; Mage, P. L.; Csordas, A. T.; Eisenstein, M.; Soh, H. T. Simultaneous elimination of carryover contamination and detection of DNA with uracil-DNA-glycosylase-supplemented loop-mediated isothermal amplification (UDG-LAMP). *Chem. Commun.* **2014**, *50*, 3747–3749.

[38] Chen, B. W.; He, Y. C.; Sung, S. Y.; Le, T. T. H.; Hsieh, C. L.; Chen, J. Y.; Wei, Z. H.; Yao, D. J. Synthesis and characterization of magnetic nanoparticles coated with polystyrene sulfonic acid for biomedical applications. *Sci. Technol. Adv. Mater.* **2020**, *21*, 471–481.

[39] Stafford, S.; Garnier, C.; Gun'ko, Y. K. Polyelectrolyte-stabilised magnetic-plasmonic nanocomposites. *Nanomaterials* **2018**, *8*, 1044.

[40] Atila Dinçer, C.; Yıldız, N.; Aydoğan, N.; Çalımlı, A. A comparative study of Fe_3O_4 nanoparticles modified with different silane compounds. *Appl. Surf. Sci.* **2014**, *318*, 297–304.

[41] Zhang, X. M.; Zhang, Q. L.; Ma, T.; Liu, Q.; Wu, S. D.; Hua, K.; Zhang, C.; Chen, M. W.; Cui, Y. L. Enhanced stability of gold magnetic nanoparticles with poly(4-styrenesulfonic acid-co-maleic acid): Tailored optical properties for protein detection. *Nanoscale Res. Lett.* **2017**, *12*, 547.

[42] Geoghegan, W. D.; Ackerman, G. A. Adsorption of horseradish peroxidase, ovomucoid and anti-immunoglobulin to colloidal gold for the indirect detection of concanavalin A, wheat germ agglutinin and goat anti-human immunoglobulin G on cell surfaces at the electron microscopic level: A new method, theory and application. *J. Histochem. Cytochem.* **1977**, *25*, 1187–1200.

[43] Carlos, F. F.; Veigas, B.; Matias, A. S.; Doria, G.; Flores, O.; Baptista, P. V. Allele specific LAMP-gold nanoparticle for characterization of single nucleotide polymorphisms. *Biotechnol. Rep. (Amst.)* **2017**, *16*, 21–25.

[44] Kwong, K. M.; Tam, C. C.; Chan, R.; Lee, S. W. L.; Ip, P.; Kwok, J. Comparison of single nucleotide polymorphism genotyping of *CYP2C19* by loop-mediated isothermal amplification and real-time PCR melting curve analysis. *Clin. Chim. Acta* **2018**, *478*, 45–50.

[45] Monroe, C.; Grier, C.; Kemp, B. M. Evaluating the efficacy of various thermo-stable polymerases against co-extracted PCR inhibitors in ancient DNA samples. *Forensic Sci. Int.* **2013**, *228*, 142–153.

[46] Connelly, C. M.; Porter, L. R.; TerMaat, J. R. PCR amplification of a triple-repeat genetic target directly from whole blood in 15 minutes as a proof-of-principle PCR study for direct sample analysis for a clinically relevant target. *BMC Med. Genet.* **2014**, *15*, 130.

[47] Liu, X. N.; Zhang, C.; Zhao, M. Y.; Liu, K. W.; Li, H.; Li, N. N.; Gao, L. L.; Yang, X. M.; Ma, T.; Zhu, J. L. et al. A direct isothermal amplification system adapted for rapid SNP genotyping of multifarious sample types. *Biosens Bioelectron.* **2018**, *115*, 70–76.

[48] Bu, Y.; Huang, H.; Zhou, G. H. Direct polymerase chain reaction (PCR) from human whole blood and filter-paper-dried blood by using a PCR buffer with a higher pH. *Anal. Biochem.* **2008**, *375*, 370–372.

[49] Kil, E. J.; Kim, S.; Lee, Y. J.; Kang, E. H.; Lee, M.; Cho, S. H.; Kim, M. K.; Lee, K. Y.; Heo, N. Y.; Choi, H. S. et al. Advanced loop-mediated isothermal amplification method for sensitive and specific detection of *Tomato chlorosis virus* using a uracil DNA glycosylase to control carry-over contamination. *J. Virol. Methods* **2015**, *213*, 68–74.

[50] Tang, Y.; Chen, H.; Diao, Y. X. Advanced uracil DNA glycosylase-supplemented real-time reverse transcription loop-mediated isothermal amplification (UDG-rRT-LAMP) method for universal and specific detection of Tembusu virus. *Sci. Rep.* **2016**, *6*, 27605.

[51] Ritzler, M.; Perschil, I.; Altwegg, M. Influence of residual uracil-DNA glycosylase activity on the electrophoretic migration of dUTP-containing PCR products. *J. Microbiol. Methods* **1999**, *35*, 73–76.

[52] Thornton, C. G.; Hartley, J. L.; Rashtchian, A. Utilizing uracil DNA glycosylase to control carryover contamination in PCR: Characterization of residual UDG activity following thermal cycling. *Biotechniques* **1992**, *13*, 180–184.

[53] Pierce, K. E.; Wangh, L. J. Effectiveness and limitations of uracil-DNA glycosylases in sensitive real-time PCR assays. *Biotechniques* **2004**, *36*, 44–46,48.

[54] Wang, H. C.; Kasper, G. Filtration efficiency of nanometer-size aerosol particles. *J. Aerosol Sci.* **1991**, *22*, 31–41.

[55] Hui, W. L.; Zhang, S. N.; Zhang, C.; Wan, Y. S.; Zhu, J. L.; Zhao, G.; Wu, S. D.; Xi, D. J.; Zhang, Q. L.; Li, N. N. et al. A novel lateral flow assay based on GoldMag nanoparticles and its clinical applications for genotyping of MTHFR C677T polymorphisms. *Nanoscale* **2016**, *8*, 3579–3587.

[56] Ouyang, Y. W.; Li, J. Y.; Haverstick, D. M.; Landers, J. P. Rotation-driven microfluidic disc for white blood cell enumeration using magnetic bead aggregation. *Anal. Chem.* **2016**, *88*, 11046–11054.